Graphical Abstract

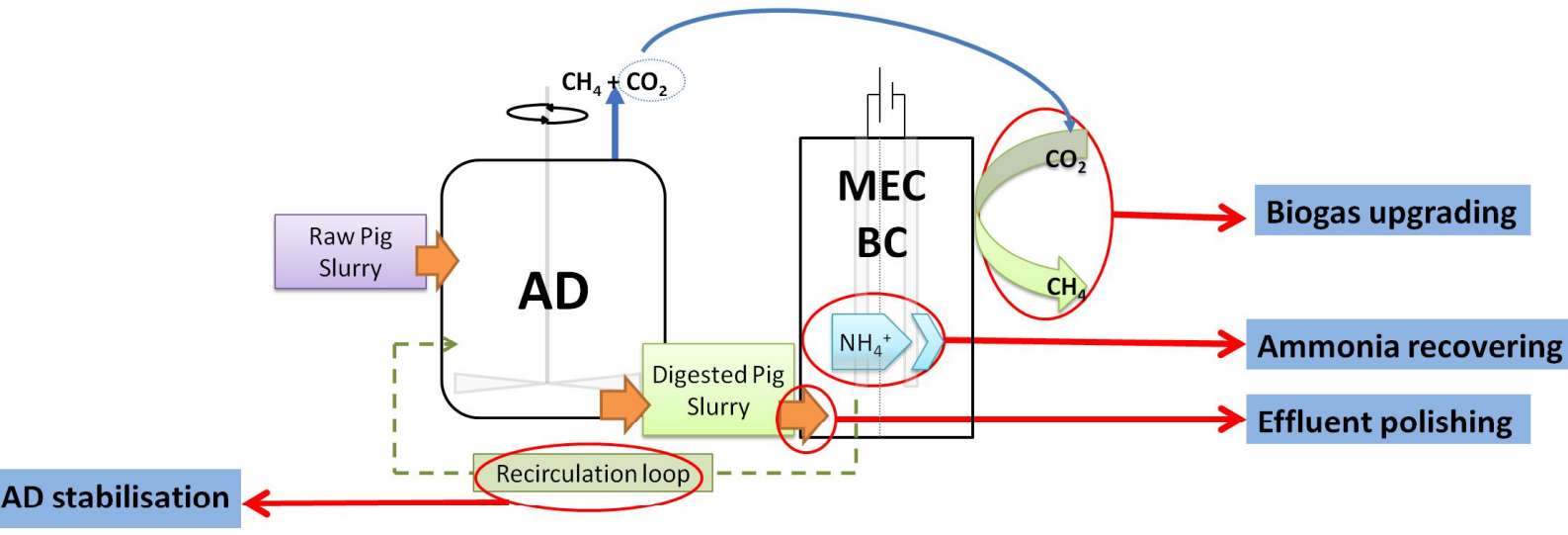

Highlights

- AD and an electromethanogenic biocathode were operated as an integrated system.
- Methane production of 79 L m^{-3} d^{-1} was achieved in the biocathode.
- Ammonium removal in the MEC anode compartment achieved 14.46 g N-NH_4^+ m^{-2} d^{-1}.
- The MEC stabilised the AD when the organic and nitrogen loading rates were doubled.

Anaerobic digestion and electromethanogenic microbial electrolysis cell integrated system: increased stability and recovery of ammonia and methane

Míriam Cerrillo[1], Marc Viñas[1], August Bonmatí[1*].

[1]IRTA. GIRO Joint Research Unit IRTA-UPC. Torre Marimon. E-08140, Caldes de Montbui, Barcelona (Spain).

* Corresponding author: A. Bonmatí, e-mail: august.bonmati@irta.cat

ABSTRACT

The integration of anaerobic digestion (AD) and a microbial electrolysis cell (MEC) with an electromethanogenic biocathode is proposed to increase the stability and robustness of the AD process against organic and nitrogen overloads; to keep the effluent quality; to recover ammonium; and to upgrade the biogas. A thermophilic lab-scale AD, fed with pig slurry, was connected in series with the bioanode compartment of a two-chambered MEC. In turn, the biocathode of the MEC was poised at -800 mV vs Standard Hydrogen Electrode and fed with CO_2 to increase the methane production of the system. After doubling its organic and nitrogen loading rate, the AD operation became stable thanks to the connection of a recirculation loop with the MEC effluent. Ammonium removal in the anode compartment of the MEC achieved 14.46 g $N\text{-}NH_4^+$ m^{-2} d^{-1}, while obtaining on average 79 L CH_4 m^{-3} d^{-1} through the conversion of CO_2 in the cathode compartment. The microbial analysis showed that methylotrophic *Methanossiliicoccaceae* family (*Methanomassiliicoccus* genus) was the most abundant among the metabolically active archaea in the AD during the inhibited state; while, on the cathode, *Methanobacteriaceae* family (*Methanobrevibacter* and *Methanobacterium* genus) shared dominance with *Methanomassiliicoccaceae* and *Methanotrichaceae* families (*Methanomassiliicoccus* and *Methanothrix* genus, respectively).

Keywords

Electromethanogenesis, biocathode, anaerobic digestion, ammonia, biogas upgrading, RNA

1. Introduction

The increasing global demand for fossil fuels, their tendency to be scarcer, and the need to control the greenhouse gas emissions when using them are requiring new strategies for energy production. An alternative to conventional refineries for clean and renewable energy production is the biorefinery. Biorefineries can recover nutrients and other products of interest from energetic crops, organic wastes and other waste fluxes [1]. This concept goes beyond the philosophy of petrochemical refineries, including sustainable management practices and closed cycle processes whenever possible. Wastes, whether domestic, industrial, agricultural or from livestock are a great opportunity to recover water, energy, chemical products and nutrients, and have a big potential for application in biorefineries [2]. Not only meeting environmental protection objectives, but also recovering energy and resources from wastes should be addressed in a circular economy [3].

The combination of anaerobic digestion (AD) and bioelectrochemical systems (BES) is an integrated strategy that can be implemented with different objectives and configurations [4, 5] and can attain the goals of the biorefinery concept [6, 7]. On the one hand, nutrients can be recovered from ammonium-rich wastewater such as pig slurry or digested pig slurry thanks to cation or anion transport through exchange membranes that takes places in BES [8]. The main example of this application is the recovery of ammonium, which can be reused as fertiliser [9-13]. Otherwise, the AD effluent would need to be processed or managed properly due to its high nutrient content. Ammonia recovery has been demonstrated in various BES including microbial fuel cells (MFCs) [10, 11] and microbial electrolysis cells (MECs) [14]. In MECs, a higher current density would greatly enhance ammonium recovery, and thus MECs exhibit a better performance for ammonium recovery than MFCs [15].

On the second hand, BES can operate with low organic loading rates and may be used to polish the effluent of the AD [16-18] or even to absorb higher organic concentrations in the digestates due to AD destabilisation or inhibition [18, 19]. Previous work has shown that integrated or multi-step systems can increase the energy production from complex substrates [4]. The combination of AD and BES for effluent polishing has been studied mainly using energy recovering MFC, to treat the effluent of a two-stage biogas process [20], digested landfill leachate [21], digested swine

wastewater [22], a digested mixture of swine manure and rice bran [23] or digested wastewater from processing potato industries [17]. Instead, the use of MEC mode proposed in this work for AD effluent polishing has been scarcely reported [19].

On the third place, the combination of the previous advantages can be applied to increase the stability of the AD process through the use of a submersible microbial desalination cell [24] or the establishment of a recirculation loop with the BES [25]. The latter strategy has proven to be effective for the control of AD inhibition due to organic and nitrogen overloads, while recovering ammonia and maintaining the effluent quality and the methane production of the AD. Other studies have reported an increased stability of the AD process when inserting electrodes in the reactor [26-28]. However, this latter configuration does not allow for ammonia recovery, as proposed in the present work.

Finally, BES have been applied to increase the methane content of the biogas produced in the AD by the use of MECs with electromethanogenic biocathodes [29, 30]. Since biogas consists mainly of methane (CH_4, 40-75%) and carbon dioxide (CO_2, 15-60%) it needs upgrading prior to its use as vehicle fuel or for injection in the natural gas grid intended to adjust the calorific. Conventional techniques for biogas upgrading focus on CO_2 removal without changing CH_4 mass [31], while electromethanogenesis performed in MEC allows for the conversion of CO_2 into CH_4 [32-34]. An alternative configuration to electromethanogenic MECs, by inserting electrodes in the AD reactor and applying a potential, allows for the in situ biogas upgrading, reporting an increase in methane yield [26, 35-37]. An increase of 59.7% in methane yield was achieved in a AD-MEC coupled system compared to the AD alone [38]. MECs for CO_2 conversion to methane have been operated mainly with synthetic medium [39, 40] and there is a lack of studies with real high strength wastewater fed for the anode compartment. The present study contributes to the body of knowledge by using a real high strength wastewater, digested pig slurry, to feed the anode compartment.

The multiple ways of AD and BES combination suggest that a more comprehensive strategy can help to settle most of the limitations of the AD process, which up to now has not been assessed. Several studies have addressed the use of BES with a combined objective, such as Zepilli et al.

[40], who operated a methane-producing MEC with a synthetic solution of soluble organic compounds, simulating the composition of a municipal wastewater, with the purpose of COD and ammonium removal, and methane production. Instead, the scientific novelty of this study was to investigate an integrated AD-MEC system fed with a high strength wastewater, such as pig slurry, and designed with a multiple purpose: i) to increase the stability and robustness of the AD process against organic and nitrogen overloads, ii) to keep the effluent quality, iii) to recover nutrients, and iv) to upgrade the biogas. None of the reported bioelectrochemical systems has simultaneously addressed these four purposes. Therefore, the application of MEC technology could be also implemented to overcome simultaneously the main limitations of AD. Furthermore, further study on the active microbial populations enriched in the bioanode and biocathode of the BES is needed to gain insight on potential resilience strategies as well as to complement previous studies [30, 40]. Until now, studies were centred on the description of the most predominant existent microorganisms on methanogenic biocathodes [29, 32, 34, 41, 42], while this study presents a novel focus on the metabolically active biomass. This novel approach bridge the gap to distinguish those active microorganisms from total microbial community in the biofilm communities in MECs.

The main aim of this study was to assess the performance of a lab-scale AD-MEC integrated system as a strategy to stabilise a pig slurry thermophilic AD under an organic and nitrogen overload, recover ammonia and increase the methane content of the biogas produced by the AD, in terms of chemical oxygen demand and ammonia removal, methane yield and energy efficiency of the process. The evolution of the active microbial community of the AD and the MEC bioelectrodes (both the anode and the cathode) was evaluated in terms of composition and activity by means of high throughput sequencing (16S rRNA *versus* 16S rDNA based Illumina-Miseq) and quantifying total and metabolically active populations (*16SrRNA* and *mcrA* gene and transcripts) by qPCR.

2. Materials and methods

2.1 Experimental set-up

A 4 L lab-scale thermophilic anaerobic continuous stirred tank reactor (AD) was used in the assays. It consisted of a cylindrical glass reactor (25 cm diameter) with a 4 L working volume. The

digester was fitted with a heat jacket with hot water circulating to keep the temperature at 55 ºC. The AD reactor was connected in series with the anode compartment of a two-chambered MEC (0.5 L in each compartment) and had a recirculation loop between both reactors. The anode of the MEC was carbon felt (dimensions: 14 x 12 cm; thickness: 3.18 mm; Alfa Aesar GmbH & Co KG, Karlsruhe, Germany) that had been inoculated with anode-inoculum from a mother MFC and had been operated with digested pig slurry as feeding solution for 9 months. The cathode chamber was filled with granular graphite with diameter ranging from 1 to 5 mm (Typ 00514, enViro-cell Umwelttechnik GmbH, Oberursel, Germany), leaving a net volume of 265 mL. Prior to being used, in order to remove metals and organic residues, the granular graphite was treated as described in Sotres et al. (2016) [43]. An A304 stainless steel mesh was used as electron collector in each compartment (dimensions: 14 x 12 cm; mesh width: 6 x 6 mm; wire thickness: 1 mm; Feval Filtros, S.L., Barcelona, Spain). The anode and cathode compartments were separated by a cation exchange membrane (CEM) (dimensions: 14 x 12 cm; Ultrex CMI-7000, Membranes International Inc., Ringwood, NJ, USA). The cathode compartment was inoculated with 30 mL of a resuspension of the anaerobic granular sludge of an UASB (volatile suspended solids content of 33 g L^{-1}) that had been operated with methanol in order to enrich the biomass in methanogenic archaea, as described elsewhere [44]. The resuspension was done by vortex mixing during 10 minutes in a 50 mL tube containing 30 g of granular sludge and 25 mL of Ringer 1/4 sterilised solution. A three electrodes configuration was used, where the anode was the counter electrode, the cathode was the working electrode and an Ag/AgCl reference electrode (Bioanalytical Systems, Inc., USA, +197 mV vs. standard hydrogen electrode (SHE)) was inserted in the cathode compartment. All potential values in this paper are referred to SHE. A potentiostat (VSP, Bio-Logic, Grenoble, France) was used for data monitoring, which was connected to a personal computer for electrode potentials and current recording every 5 min using EC-Lab software (Bio-Logic, Grenoble, France). The anode was fed with filtered digested pig slurry (125 µm) from the AD and the cathode compartment was fed with a synthetic solution which contained (per litre of deionised water): 5 g L^{-1} of $NaHCO_3$, NH_4Cl, 0.87 g; $CaCl_2$, 14.7 mg; KH_2PO_4, 3 g; Na_2HPO_4, 6 g; $MgSO_4$, 0.246 g; and 1 mL L^{-1} of a trace elements solution as described elsewhere [45].

2.2 Reactor operation

The AD was fed with pig slurry (Table 1) and operated for 222 days in three different phases, with a hydraulic retention time (HRT) of 10 days (Table 2). In Phase 1, the organic loading rate (OLR) and nitrogen loading rate (NLR) were established at 3.92 kg_{COD} m^{-3} day^{-1} and 0.22 kg_N m^{-3} day^{-1}, respectively. In Phase 2, the OLR and NLR were doubled to force the inhibition of the reactor [25]. And finally, in Phase 3, keeping the OLR and NLR equal to Phase 2, a recirculation loop with the MEC was connected (50% of the AD feed flow rate) to recover the AD. Samples of the AD effluent were taken once a week in order to assess the operation of the reactor.

The MEC was operated in continuous in series with the AD poising the cathode potential at -800 mV *vs* SHE. The solutions of both the anode and the cathode compartment were fed in continuous at 20 mL h^{-1} and mixed by an external pump. The HRT was of 32.4 h and 14.1 h for the anode and cathode compartment, respectively (with respect to the net volume of each compartment), with an OLR and NLR of the anode compartment for each phase specified in Table 2. The MEC was operated at room temperature during the entire assay (23±2 ºC).

Table 1. Characterisation of the raw pig slurry used as feeding solution in the anaerobic digester (AD) in Phase 1 and Phases 2 and 3 (n=number of samples; mean±standard deviation).

Parameter	**Raw pig slurry**	
	Phase 1 (n=6)	**Phase 2 and 3** (n=12)
pH (-)	7.1±0.1	6.8±0.2
COD (g_{O2} kg^{-1})	43.96±2.04	80.55±6.40
NTK (g L^{-1})	2.41±0.00	4.29±0.17
$N\text{-}NH_4^+$ (g L^{-1})	1.59±0.08	2.97±0.25
TS (g kg^{-1})	24.40±0.52	47.95±2.53
VS (g kg^{-1})	16.37±0.43	32.79±1.88

Table 2. Operational conditions for the AD reactor and the MEC (mean±standard deviation).

Phase	**Period (d)**	**AD**			**MEC**	
		OLR (kg_{COD} m^{-3} d^{-1})	**NLR (kg_N m^{-3} d^{-1})**	**Recirculation (% feed flow rate)**	**OLR (kg_{COD} m^{-3} d^{-1})**	**NLR (kg_N m^{-3} d^{-1})**
1	1 - 78	3.92±0.61	0.22±0.03	0	7.87±0.76	0.74±0.04
2	78 - 126	7.39±1.36	0.40±0.06	0	43.12±3.58	2.42±0.13
3	126 - 222			50		

160 **2.3. Analytical methods and calculations**

161 Samples were analysed for pH, chemical oxygen demand (COD) and ammonium ($N\text{-}NH_4^+$)
162 according to Standard Methods 5220 [46]. Methane content of the biogas produced by the AD was
163 analysed using a gas chromatograph (CP-3800, Varian, USA). Methane was measured (through
164 the determination of dissolved methane) in the cathode samples according to Henry's Law and the
165 following method [47]. Around 2 mL catholyte samples were collected with a 5 mL syringe and
166 injected with a needle in a 4 mL vacutainer. The vacutainers were shaken vigorously for 30 s and
167 then allowed to stand for 1 h. Headspace gas was analysed for CH_4 using a gas chromatograph
168 (CP-3800, Varian, USA). Dissolved CH_4 was computed using the equation:

169

$$X_L = \frac{C_{CH_4} \cdot MV_{CH_4} \cdot MW_{CH_4} \cdot (V_T - V_L + \propto V_L) \cdot 1000}{V_L} \quad (1)$$

170

171

172

173 where X_L is the concentration of CH_4 (mg L^{-1}) in the solution, C_{CH4} is the concentration of CH_4 (%)
174 in the headspace 1 h after shaking, MV_{CH4} is the molar volume of CH_4 at 25 ºC (0.041 mol L^{-1}),
175 MW_{CH4} is the molecular weight of CH_4 (16 g mol^{-1}), V_T is the volume (mL) of the vacutainer, V_L is
176 the volume (mL) of the solution, and α is the water:air partition coefficient at 25 ºC (0.03). Methane
177 production was normalised to the net volume of the cathode compartment (0.265 L).
178 Partial alkalinity (PA, titration from the original pH sample to pH 5.75, an alkalinity which
179 corresponds roughly to bicarbonate alkalinity) and total alkalinity (TA, titration to pH 4.3) were
180 determined to obtain intermediate alkalinity (IA, titration from 5.75 to 4.3, approximately the VFA
181 alkalinity) [48]. The IA:TA ratio was used as a tool to monitor anaerobic digestion, considering that
182 the process was stable when the IA:TA was below 0.3 [49]. COD and ammonium removal
183 efficiency in the MEC was calculated as the ratio of the difference between anode influent and
184 effluent concentrations and the influent concentration [25].

185 **2.4. Electrochemical measurements and calculations**

186 The current density (A m^{-2}) of the MEC was calculated as the quotient between the intensity
187 recorded by the potentiostat (A) and the area of the anode (m^2). The Coulombic efficiency (CE), or

the fraction of electrons obtained from the consumption of COD that are available for methane production at the cathode was calculated as:

$$CE = \frac{M \int_0^t I\,dt}{F\,b\,q\,\Delta COD} \quad (2)$$

The energy efficiency relative to electrical input recovered as methane (EE_e, Equation 3), the energy efficiency relative to the energy content of the substrate (EE_s, Equation 4) and the energy efficiency with respect to the energy input and the energy in the substrate (EE_{e+s}, Equation 5) were:

$$EE_e = \frac{n_{CH_4}\,\Delta G_{CH_4}}{\int_0^t I\,E_{ap}\,dt} \quad (3)$$

$$EE_s = \frac{n_{CH_4}\,\Delta G_{CH_4}}{n_S\,\Delta G_S} \quad (4)$$

$$EE_{e+s} = \frac{n_{CH_4}\,\Delta G_{CH_4}}{\int_0^t I\,E_{ap}\,dt + n_S\,\Delta G_S} \quad (5)$$

where M is the molecular weight of the final electron acceptor, I is the current (A), F is Faraday's constant (96485 C mol^{-1}), b is the number of electrons transferred per mole of O_2, q is the volumetric influent flow rate (L d^{-1}), ΔCOD is the difference in the influent and effluent COD, n_{CH4} are the moles of produced methane, ΔG_{CH4} is the molar Gibbs free energy of CH_4 oxidation by oxygen to carbon dioxide (-817.97 kJ mol^{-1}), E_{ap} is the applied voltage calculated as the difference between the cathode and anode potentials (V), n_S are the moles of acetate consumed and ΔG_S is the molar Gibbs free energy of acetate oxidation to carbon dioxide (-844.61 kJ mol^{-1}).

Finally, the cathodic methane recovery efficiency (R_{cat}), defined as the fraction of electrons reaching the cathode that are recovered as methane, was calculated as:

$$R_{cat} = \frac{8\,F\,n_{CH_4}}{\int_0^t I\,dt} \quad (6)$$

Cyclic voltammetries (CV) in turnover conditions, i.e. in the presence of substrate, were performed using a potentiostat (VSP, Bio-Logic, Grenoble, France) after the cathode inoculation (day 0) and at the end of Phase 2 and 3 (day 78 and 222 of the assays, respectively), in order to study the

electroactive microbial biofilm developed on the cathode. The same three-electrode configuration used for the MECs operation was maintained for the set up of the CV. The start (E_i) and vertex (E_f) potentials were -800 and +400 mV *vs* SHE, respectively, and the scan rate was set at 1 mV s^{-1}.

2.5. Microbial community analysis

The bacterial communities in the biofilm harboured in the bioanode and the biocathode of the MEC at the end of Phase 2 and 3 and in the AD biomass at the end of each Phase (1, 2 and 3) were analysed by culture-independent molecular techniques such as quantitative PCR (qPCR) and high throughput sequencing (MiSeq, Illumina) of partial *16S* rDNA and *16S* rRNA massive libraries. To stabilise the nucleic acid, especially RNA, samples were stored at -80 ºC. The inoculum of the cathode and the biofilm settled up on the anode had been characterised in previous work [44, 50]. Briefly, regarding eubacteria, the cathode inoculum was dominated by *Bacteroidetes*, *Firmicutes* and *Synergistetes* (61, 14 and 8%, respectively); *Methanosarcinaceae* (52%) was the predominant archaea family (methylotrophs genus, *Methanomethylovorans* and *Methanolobus*) [44]. In the case of MEC anode biofilm, *Firmicutes, Bacteroidetes* and *Proteobacteria* were the dominant eubacterial *phyla* (35, 30 and 11%, respectively), and the predominant archaea family was *Methanotrichaceae*, (87%) [44, 50].

2.5.1 Nucleic acid extraction and cDNA synthesis

Simultaneous total genomic DNA and RNA (including rRNA) were extracted in triplicate from known weights of each sample, which consisted in effluent from the AD, a piece of carbon felt from the anode (1 cm^2) and granular graphite collected from the cathode compartments for the biocathode biofilm. The PowerMicrobiome™ RNA Isolation Kit (MoBio Laboratories Inc., Carlsbad, CA, USA) was used according to manufacturer's instructions, and cDNA was obtained from total RNA following the protocol described elsewhere [50]. Henceforth, the term cDNA or *16S* rRNA is used to refer to the extracted RNA or 16S transcripts as amplicons from cDNA as a measure of gene expression and microbial activity, whereas DNA or *16S* rDNA terms are used referring to the extracted genomic DNA and 16SrDNA amplicons from DNA.

240 **2.5.2 Quantitative PCR assay (qPCR)**

241 Total gene copy numbers and gene transcripts of eubacterial *16S rRNA* gene and *mcrA* gene
242 (methanogenic archaeal methyl coenzyme-M reductase) were quantified by means of qPCR. Each
243 sample was analysed in triplicate by means of the three independent DNA and RNA (cDNA)
244 extracts. The analysis was carried out following the protocol described elsewhere [25]. The
245 standard curve parameters of the qPCRs were as follows (for *16S* rRNA and *mcr*A, respectively): a
246 slope of -3.244 and -3.532; a correlation coefficient of 0.998 and 0.999; and an efficiency of 103
247 and 92%.

248 **2.5.3 High throughput sequencing and data analysis**

249 Simultaneous DNA and RNA (cDNA) extracts obtained from the AD and the bioanode and
250 biocathode biofilm, used for qPCR analysis, were also assessed by 16SrRNA gene based- MiSeq,
251 following the specific steps described elsewhere [25]. The Bayesian Classifier tool of the
252 Ribosomal Database Project (RDP) was used to taxonomically classify the obtained Operational
253 Taxonomic Units (OTUs) [51]. The data obtained from sequencing datasets for eubacterial and
254 archaeal populations was submitted to the Sequence Read Archive of the National Center for
255 Biotechnology Information (NCBI) under the study accession number SRP072956.

256 A statistical multivariate analysis by means of correspondence analysis (CA) on the OTUs
257 abundance matrix of Eubacterial *and* Archaeal was performed. The obtained samples and OTUs
258 scores were depicted in a 2D biplot, which represented the phylogenetic assignment of the
259 predominant OTUs (relative abundance above 1 %). The diversity of the samples was evaluated
260 with the number of OTUs, the inverted Simpson index, Shannon index and Goods coverage using
261 the Mothur software v.1.34.4 (http://www.mothur.org) [52], normalising all the estimators to the
262 lowest number of reads among the different samples.

263

264 **3. Results and discussion**

265 **3.1 Performance of the AD (Phase 1 and Phase 2)**

266 The AD showed a stable operation during Phase 1 (Figure 1), with an average COD removal
267 efficiency of 54±8% and a methane production of 0.45±0.06 m^3 m^{-3} d^{-1} (Table 3). The IA:TA ratio

was kept below 0.3, corroborating the stability of the reactor. When the OLR and NLR of the AD were doubled in Phase 2, the reactor showed a fast inhibition, reducing the value of COD removal to 18% and the methane production to 0.23 m^3 m^{-3} d^{-1}, 50% of the obtained in the previous phase (Figure 1a and b). VFA accumulated, reaching values of 5670 mg L^{-1} for acetate, 1850 mg L^{-1} for propionate and over 1000 mg L^{-1} for butyrate (Figure 1c), and the IA:TA ratio increased to 0.44 (Figure 1d) confirming the instability of the AD reactor.

Table 3. Summary of the main parameters for the AD and the MEC reactors in the different phases. Results for the AD correspond to the stable period of each phase (mean±standard deviation).

Parameter	Phase 1	Phase 2	Phase 3
AD			
CH_4 production (m^{-3} m^{-3} d^{-1})	0.45±0.06	0.27±0.04	0.38±0.04
COD removal efficiency (%)	54±8	28±8	22±5
IA:TA	0.22±0.04	0.40±0.08	0.50±0.03
pH	7.8±0.1	7.8±0.1	7.6±0.1
MEC			
COD removal efficiency (%)	24±8	14±5	21±6
N-NH_4^+ removal efficiency (%)	30±6	18±5	20±5
CE (%)	3.5±1.8	2.1±1.4	1.5±0.5
CH_4 production (L m^{-3} d^{-1})	79±34	63±15	78±29
R_{cat} (%)	45±37	61±18	59±13
EE_e (%)	50±41	62±17	85±23
EE_s (%)	4.2±2.3	3.0±1.5	1.4±0.7
EE_{e+s} (%)	3.6±1.4	2.9±1.4	1.4±0.7
Energy input (kWh m^{-3}_{CH4})	39±33	15.8±4.5	11.5±3.4
AD-MEC			
COD removal efficiency (%)	-	42±6	41±6

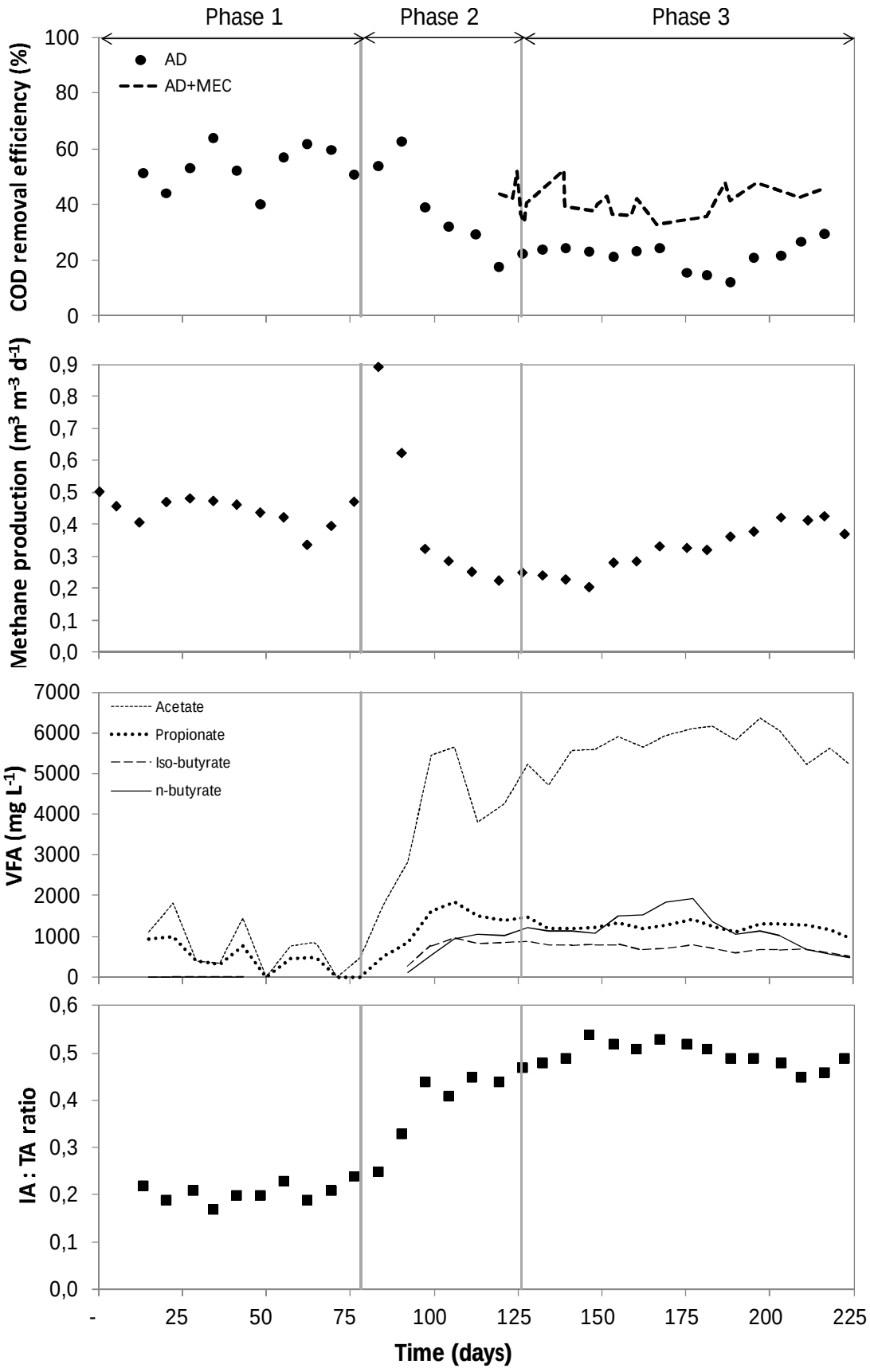

Figure 1 Performance of the AD regarding (a) COD removal efficiency; (b) methane production; (c) VFA concentration; and (d) IA:TA ratio.

3.2 Performance of the MEC (Phase 1 and Phase 2)

The MEC fed with the effluent of the AD during Phase 1 showed a stable performance regarding current density production during the first 30 days of operation (Figure 2), with an average current density of 0.4 A m^{-2}. Afterwards, the current density production became instable, showing peaks of up to 4.5 A m^{-2} (average of 1.5 A m^{-2}) and was drastically reduced from day 64 onward due to the degradation of the stainless steel mesh used as electron collector in the anode compartment (data corresponding to the instable period was not considered for calculations). The mesh was replaced at the beginning of Phase 2. This change produced some period of instability at the beginning of Phase 2, but afterwards the MEC showed a current density production similar to the obtained in Phase 1. The COD removal efficiency of the MEC in Phase 1 was of 24±8%, with a maximum removal of 3.2 kg_{COD} m^{-3} d^{-1}, and the CE was of 3.5±1.8% (Table 3). In Phase 2 the COD removal efficiency and the CE decreased to 14±5% and 2.1±1.4%, respectively. Since CE is related with the substrate concentration, the increase in COD of the influent resulted in a decrease in CE [53].The ammonium removal efficiency in Phase 1 was of 30±6%, corresponding to 6.64 g $N\text{-}NH_4^+$ m^{-2} d^{-1}. The removal efficiency decreased to 18±5% during Phase 2, although the absolute flux was higher (12.87 g $N\text{-}NH_4^+$ m^{-2} d^{-1}) as a result of the increased NLR. Previous work performed with the same MEC but with an abiotic cathode fed with NaCl (0.1 g L^{-1}) and higher organic and nitrogen loading rates (28.50±1.80 kg_{COD} m^{-3} day^{-1} and 1.73±0.09 kg_N m^{-3} day^{-1}, respectively) achieved a nitrogen removal rate of 12.97±2.04 g $N\text{-}NH_4^+$ m^{-2} d^{-1}, similar to the one obtained in Phase 2 and almost doubling the rate obtained in Phase 1 in this study [25]. And values as high as 86 g $N\text{-}NH_4^+$ m^{-2} d^{-1} were reported with a submersible microbial desalination cell fed with synthetic solution [24].

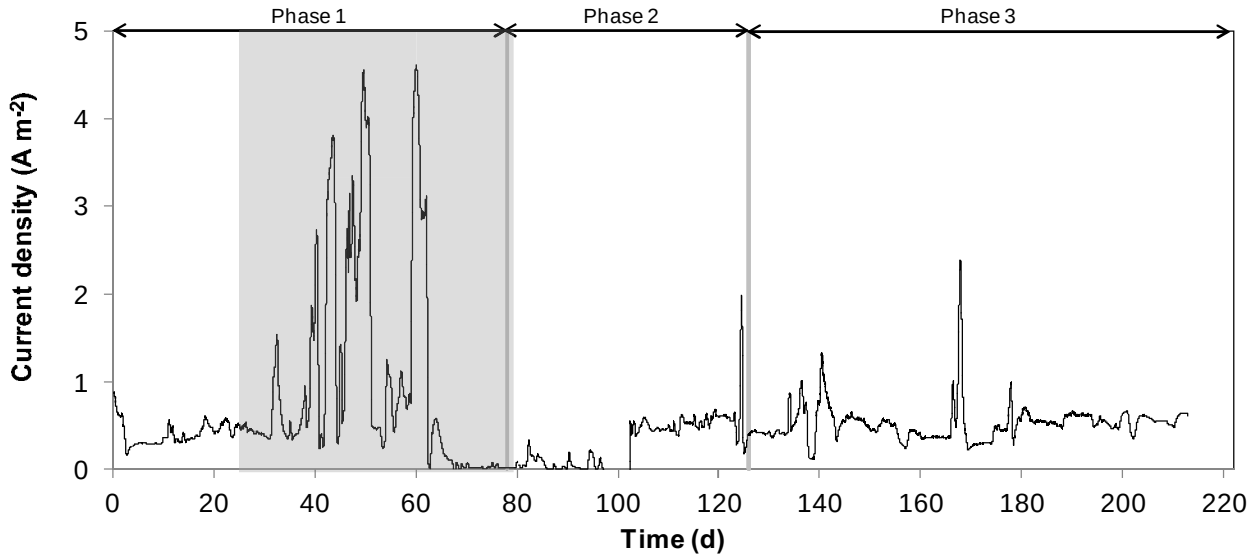

Figure 2 Current density profile obtained during the operation of the MEC. Data corresponding to the instable period (shaded) was not considered for calculations.

3.3 Performance of the AD-MEC combined system with recirculation loop (Phase 3)

When the recirculation loop with the MEC was connected in Phase 3, the performance of the AD started to recover, with COD removal values achieving 30% (below 20% in the end of Phase 2) and a maximum methane production of 0.43 m^3 m^{-3} d^{-1}, representing a 100% increase with respect to the production at the end of Phase 2, and nearly recovering the values achieved in Phase 1. However, the VFA concentration and the IA:TA ratio were similar to the previous phase. Interestingly, the overall performance of the AD-MEC integrated system maintained the COD removal in a range of 33-52%, in spite of the poorer performance of the AD, concomitant to an ammonium removal of 20±5% (14.46 g $N\text{-}NH_4^+$ m^{-2} d^{-1}). The MEC showed a current density production similar to the obtained at the beginning of Phase 1. The CE of the MEC decreased with respect to Phase 1, as described in Phase 2. The low CEs obtained are to be expected when working with complex substrates where other electron acceptors may be present [54-56]. Much higher CEs have been previously reported, such as 72-80% [40].

3.4 Biocathode operation performance

Methane production in the cathode compartment was around 0.079 m^3 m^{-3} d^{-1}. A volume of biogas of 0.2 m^3 m^{-3} d^{-1} could be treated in this MEC with biocathode, assuming a typical biogas

composition of 60% CH_4 and 40% CO_2 (490.78 kJ mol^{-1}) to obtain methane with a purity prochain to 100% (817.97 kJ mol^{-1}) Higher methane productions have been achieved in previous works, such as 0.16 m^3 m^{-3} d^{-1} [39], or 0.28 m^3 m^{-3} d^{-1} [57].

The highest R_{cat} was achieved in Phase 2 (61±18%), although the high variability of the obtained results makes the observed differences between phases not to be significant (Table 3). A recent review on bioelectrochemical power-to-gas, collected R_{cat} of previous studies between 19 to 156%, were values >100% were likely the result of microbially influenced corrosion of the cathode by methanogens [58]. The obtained results for R_{cat} in the present study are below the 96% previously reported by Cheng et al. (2009) [32], the 84-86% obtained by Zeppilli et al. (2014) [40], or the 69% reported by Batlle-Vilanova et al. (2015) [30]. But they are much higher than the 23.1% achieved by Van Eerten-Jansen et al. (2001) [59] or the 24.2 ± 4.7% reported by Zhen et al. (2015) [42].

The EEe was between 50 and 85%, values similar to the obtained in batch mode with a two-chambered MEC using graphite granules as electrodes (57%) [33]. The low CE achieved in this MEC made also the obtained EEs (between 1.4 and 3.6%) to be low in comparison with the previous work (between 23 and 54%).

Figure 3 shows the cyclic voltammograms obtained after the cathode inoculation and at the end of Phases 2 (78 days) and 3 (222 days). The curve obtained at the start of the operation showed a low response to the different applied potentials, as a result of the recent inoculation. The performance of the biocathode increased at the voltage of -800 mV at the end of the assay (Phase 3), coincidently with the period of the best EE_e.

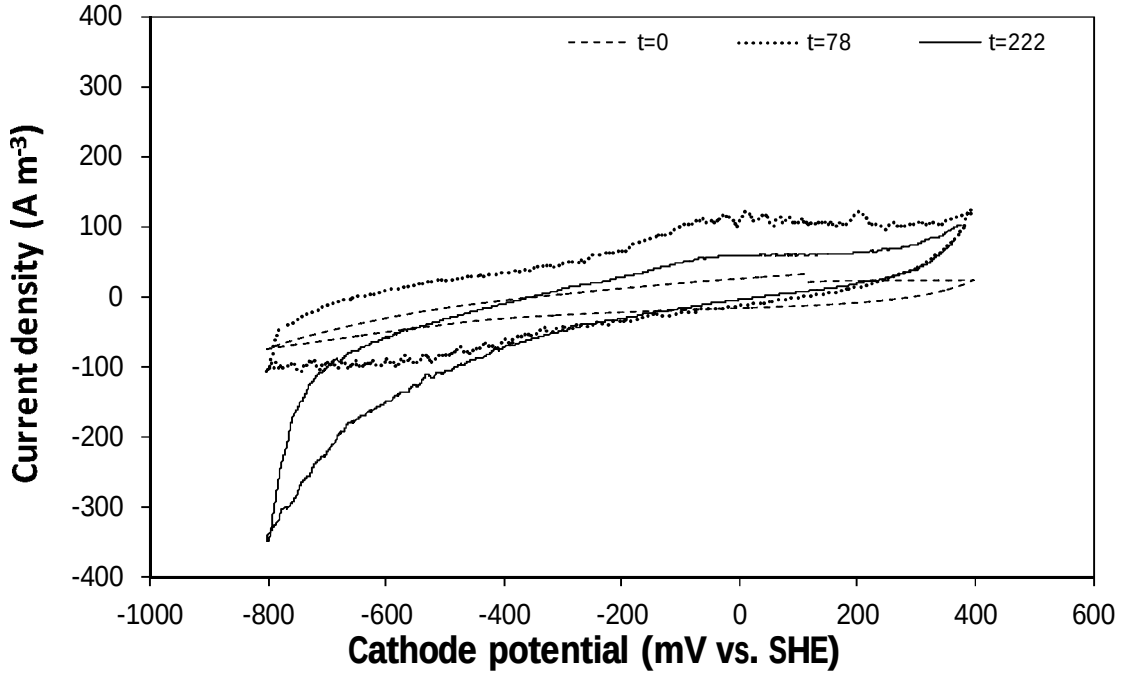

Figure 3 Cyclic voltammograms of the MEC after the cathode inoculation (t=0 d) and at the end of Phase 2 and 3 ((t=78 d and t=222 d, respectively).

3.5 Considerations about biogas upgrading and ammonia recovery application

In dual-chamber MECs for methane production, water is usually used for electron donor in the anode chamber, since it is a widely available and cheap source [60]. However, the electric energy input is considerable higher compared to a BES using wastewater oxidation in the bioanode [58]. In this study, the average energy input for biomethane production from CO_2 in the biocathode in Phase 3 was 11.5±3.4 kWh m^{-3} (Table 3). In a previous work, Van Eerten-Jansen et al. [59] achieved an energy input of 73.5 kWh m^{-3} in an electromethanogenic biocathode operated in continuous with water as electron donor. The energy input was reduced to 15.4 kWh m^{-3} following the oxidation of hexacyanoferrate (II).

The values of electricity consumption obtained in this studies are similar to the ones corresponding for conventional biogas upgrading technologies, such as pressure swing adsorption (0.25 kWh m^{-3}), water scrubbing (<0.25 kWh m^{-3}), organic physical scrubbing (0.24-0.33 kWh m^{-3}) or chemical scrubbing (<0.15 kWh m^{-3}) [61]. It is noteworthy that these values refer to the volume of biogas

364 treated, not to the volume of methane produced, as the previous ones. Furthermore, conventional
365 technologies are based on CO_2 removal, instead of CO_2 conversion to CH_4 proposed in this study.
366 Finally, it is noteworthy that the energy consumption of the MEC is not only invested in methane
367 production, but also used for ammonia recovery. The energy consumption for this latter aim
368 represented on average 3 kWh $kg^{-1}_{Nrecovered}$, while the values reported for conventional techniques
369 for ammonia removal range are 13 kWh $kg^{-1}_{N\ removed}$ in a nitrification denitrification process, 5 kWh
370 $kg^{-1}_{N\ removed}$ in a Sharon-Anammox process, or 9 kWh $kg^{-1}_{N\ recovered}$ in NH_3 stripping [62].
371 There are still many challenges to overcome in order for AD-MEC coupled system with
372 electromethanogenic biocathode to be applied in large scale systems for biogas upgrading and
373 ammonia recovery. Mainly, the use of phosphate buffer in the cathode compartment to avoid pH
374 increase is not a sustainable approach for scaled systems [7] and an alternative should be
375 implemented. Furthermore, the use of the buffer hinders the recovery of ammonia by stripping of
376 the catholite and adsorption that has been used in previous work [25].

377 **3.6. Microbial community assessment**

378 The microbial community structure and activity of the samples taken from the AD and the biofilm
379 harboured on the electrodes of the MEC was characterised by means of qPCR technique and
380 sequenced by MiSeq.

381 **3.6.1 Quantitative analysis by qPCR**

382 Figure 4 shows qPCR results for *16S* rRNA and *mcr*A gene copy numbers of the seven samples
383 analysed, either for DNA (present microorganisms) and cDNA (active microorganisms). In the AD
384 samples eubacteria remained in the same order of magnitude for *16S* rRNA gene copy numbers g^{-1}
385 during the stable, inhibited and recovered states; while showed a decrease of one order of
386 magnitude for *mcr*A (from $1.26 \cdot 10^8$ to $2.18 \cdot 10^7$ gene copy numbers g^{-1}) at the end of Phase 2 due
387 to the inhibition caused by doubling the OLR and NLR. The connexion of the recirculation loop
388 reduced the inhibition and helped to recover the methanogenic population, returning to levels
389 similar to those existing prior to the inhibition ($1.38 \cdot 10^8$ gene copy numbers g^{-1}). The same
390 behaviour was observed at cDNA-based qPCR, showing a decrease of one order of magnitude for
391 *mcr*A transcripts copy numbers in the AD sample of the end of Phase 2 and corroborating that the

methanogenic population was suffering inhibition. The magnitude of the reduction in *mcr*A gene copy numbers when the AD was submitted to inhibition by an organic and nitrogen overload was similar to the described in previous work [50, 63]. In Phase 1 free ammonia nitrogen (FAN) concentration was in the range of 400-670 mg L^{-1}. Concentrations of FAN above 900 mg L^{-1} were reached during Phase 2, when the OLR and NLR were doubled, with a maximum of 1186 mg FAN L^{-1} at the end of the Phase. At these levels the first signs of inhibition may occur according to previous studies [64, 65]. Once the recirculation loop was established in Phase 3, FAN levels remained in a range of 365-740 mg L^{-1}.

Regarding the MEC, gene copy numbers for *16S* rRNA for the anode and cathode biofilm were of the same order of magnitude both for Phase 2 and 3 samples, either in DNA or in cDNA forms. On the contrary, *mcrA* gene copy numbers of the anode sample increased at the end of the recirculation phase, probably due to the parallel increase of methanogenic population in the AD. In the case of the cathode biofilm, *mcrA* gene copy numbers g^{-1} for DNA-based qPCR at the end of the assay were within 10^6 gene copy numbers g^{-1}, coincidently with the values obtained in a previous work with methanogenic biofilm harboured by granular graphite [30]. While a total methanogenic population decrease was observed from the initial cathode to the final sample (DNA level), *mcrA* expression belonging to methanogenic archaea increased one order of magnitude (from $1.40 \cdot 10^5$ to $2.63 \cdot 10^6$ transcript copy numbers g^{-1}).

From these results, it is clear that the AD methanogenic population decreased due to the organic and nitrogen overload and then could be recovered thanks to the establishment of the recirculation loop with the MEC. Furthermore, the methanogenic cathode of the MEC was progressively enriched in metabolically active methanogenic archaea.

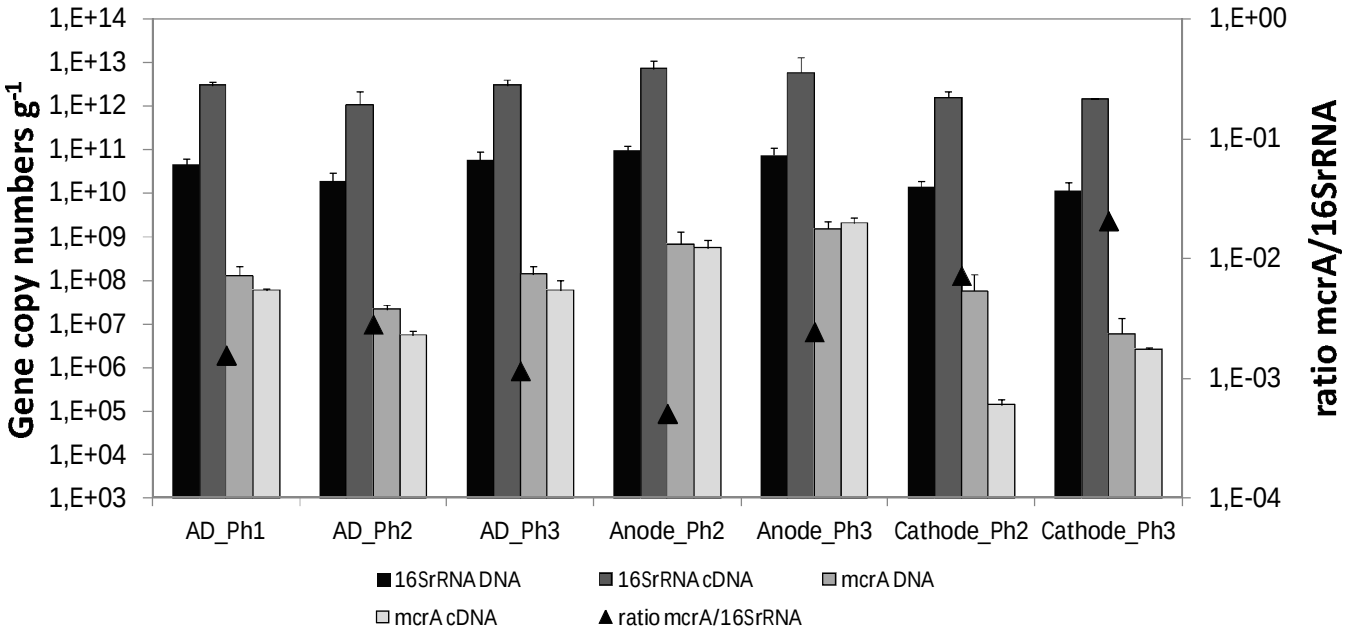

415

416 **Figure 4** Gene copy numbers for *16S* rRNA and *mcr*A genes and ratio between them of DNA
417 and cDNA, of the AD effluent at the end of Phases 1, 2 and 3, and the biofilm harboured on the
418 anode and cathode of the MEC at the end of Phase 2 and 3.

419

420 **3.6.2 High Throughput Sequencing (16S-based MiSeq) results for eubacteria and archaea**

421 Table 4 shows the number of reads obtained for the AD samples and the anode and cathode
422 biofilms of the MEC for eubacteria (6822 OTUs) and archaea (900 OTUs). Figure 5a shows the
423 relative abundance of eubacterial *phyla* for the seven samples, regarding DNA (present
424 microorganisms) and cDNA (metabolically active microorganisms) forms. The three AD samples
425 showed a similar eubacterial composition at DNA level, dominated by *Firmicutes*, *Bacteroidetes*
426 and *Proteobacteria*, with relative abundances in the ranges of 64-68%, 12-18% and 5-10%,
427 respectively. Previous studies, performed also in a thermophilic AD running on pig slurry, found
428 that the *Firmicutes phylum* was the predominant one [25, 66]. The sample from the end of Phase 2
429 showed a decrease in *Firmicutes* and *Proteobacteria phyla* with respect to Phase 1 and the sample
430 at the end of Phase 3, while *Bacteroidetes* increased slightly. At cDNA level, although *Firmicutes*
431 was still the predominant *phylum* (46-75% of relative abundance), *Proteobacteria* active
432 microorganisms clearly surpassed *Bacteroidetes* (19-40% and 1-5%, respectively) and were
433 increasingly more abundant over time, while *Firmicutes* showed the opposite tendency.

434 *Bacteroidetes* was the predominant *phylum* in the anode of the MEC both in Phase 2 and 3
435 samples (34 and 41%, respectively), according to DNA-based sequencing, while *Proteobacteria*
436 revealed as the most active one in Phase 2 sample (65%) and *Bacteroidetes* and *Proteobacteria*
437 shared dominance in the final sample (18 and 16%, respectively). These three phyla have been
438 identified in previous studies in BES [67, 68]. In the case of the cathode biofilm, the domination of
439 *Firmicutes* at DNA level in Phase 2 and 3 samples (56 and 31%, respectively), shared by
440 *Proteobacteria* in Phase 3 sample (33%), shifted to a clear dominance of *Proteobacteria* in both
441 samples at cDNA level (59 and 68%).
442 At family level *Clostridiaceae 1* and *Peptostreptococcaceae* were the most present and active
443 groups in the three AD samples (Figure 5b). *Porphyromonadaceae*, which was the third more
444 abundant family (6-9%) at DNA level, showed a low activity according to cDNA sequencing (below
445 1%). *Planococcaceae* and *Pseudomonadaceae* revealed as active families at the end of Phase 2
446 (21 and 12%, respectively), as *Campylobacteraceae* at the end of Phase 2 (13%), although they
447 were below 3% in DNA form abundance. Regarding the samples of the MEC anode,
448 *Planctomyceraceae* and *Porphyromonadaceae* stood out in the Phase 2 sample when looking at
449 DNA sequencing results (12 and 16%, respectively), but were replaced by *Desulfuromonadaceae*
450 and *Pseudomonadaceae* families according to cDNA (21 and 18%, respectively). In Phase 3
451 anode sample Porphyromonadaceae and Planctomycetaceae were the most abundant families at
452 DNA (12%) and cDNA (14%) levels, respectively. Finally, the cathode biofilm was dominated by
453 *Clostridiaceae* in Phase 2 and 3 samples at DNA level (34 and 12%, respectively), but by
454 metabolically active *Phodocyclaceae* and *Desulfovibrionaceae* according to cDNA results (14 and
455 37%, respectively). Thus, a clear differentiation between total eubacteria and active eubacterial
456 microorganisms, especially in the biomass harboured by the MEC electrodes, has been shown.
457 Figure 5c shows the relative abundance of archaea families of the seven samples. Although
458 *Methanobacteriaceae* showed a high abundance in the three AD samples (74-86%), the most
459 active archaeal populations were *Methanomicrobiaceae* in Phase 1 and Phase 3 AD samples (58
460 and 56%, respectively) and Methanossiliicoccaceae in Phase 2 sample (54%). Members of
461 *Methanomassiliicoccaceae* family have recently been described as obligate hydrogen-consuming

462 methanogens, reducing methanol and methylamines instead of carbon dioxide [69, 70]. A recent
463 study has reported an increase of this family at high OLR, and concluded that an additional
464 methanogenic pathway might contribute to methane production at high OLR [71]. It has also been
465 reported that this family emerged in the recovery process of a thermophilic AD after an organic
466 overload [72], since methanol could be produced fermentatively from lactate by a kind of
467 *Clostridium* species. Methanogenic population in the AD showed higher differences between
468 existing vs active composition than eubacteria. On the contrary, *Methanotrichaceae*, the
469 predominant family on the MEC anode Phase 2 and Phase 3 samples in presence (75 and 48%,
470 respectively) was also active (74 and 31%, respectively), independently of being on a low relative
471 abundance in the AD. On the other hand, *Methanossiliicoccaceae* and *Methanomicrobiaceae*
472 increased in presence and activity over time, probably due to the high activity of these families in
473 the AD. When looking at the cathode biofilm, *Methanotrichaceae* (genus *Methanothrix*, formerly
474 known as *Methanosaeta*) was the dominant family at the Phase 2 sample either in presence and
475 activity (53 and 68%, respectively), while in the Phase 3 sample it dominated at DNA but not at
476 cDNA level (36% and 0.3%, respectively). *Methanotrix* (*Methanosaeta) genus* was also detected in
477 a methanogenic cathode by Xu et al. (2014) [29] and Cai et al. (2016) [73]. It has been recently
478 described that *Methanotrix (Methanosaeta)* is capable of accepting electrons via direct interspecies
479 electron transfer (DIET) for the reduction of carbon dioxide to methane [74], so a deeper study is
480 necessary to understand the role of these species in the cathode biofilm of the methanogenic
481 MEC. *Methanomassiliicoccaceae* (genus *Methanomassiliicoccus*) and *Methanobacteriaceae*
482 (genus *Methanobacterium* and *Methanobrevibacter*) were also families with high relative
483 abundances at DNA level (15-31%), being the most active ones in the Phase 3 sample (57 and
484 33%, respectively) as well. Previous works have showed a clear dominance of
485 *Methanobacteriaceae* family in methanogenic biocathodes [29, 32, 34, 41, 42], differing from the
486 results obtained in this study. The high relative abundance of the methylotrophic
487 *Methanomassiliicoccaceae* family among the active archaea suggests that methanol must be
488 present in the cathode compartment, although it was not monitored in the present study. Methanol
489 produced in the anode compartment due to the fermentation of organic compounds could migrate

to the cathode compartment through the CEM. Methanol could be also produced at very low O_2 partial pressure, from methane by ammonia oxidising bacteria (AOB) which can partially oxidise CH_4 to methanol when using ammonia as an energy source [75]. The genera *Nitrosomonas*, a well known AOB, was present in the biocathode samples, although at low relative abundance (<0.01%). Besides, some methane oxidising archaea and bacteria can also carry out anaerobic oxidation of methane [76], although so far they are poorly known and it cannot be determined if they are present in the biocathode.

a)

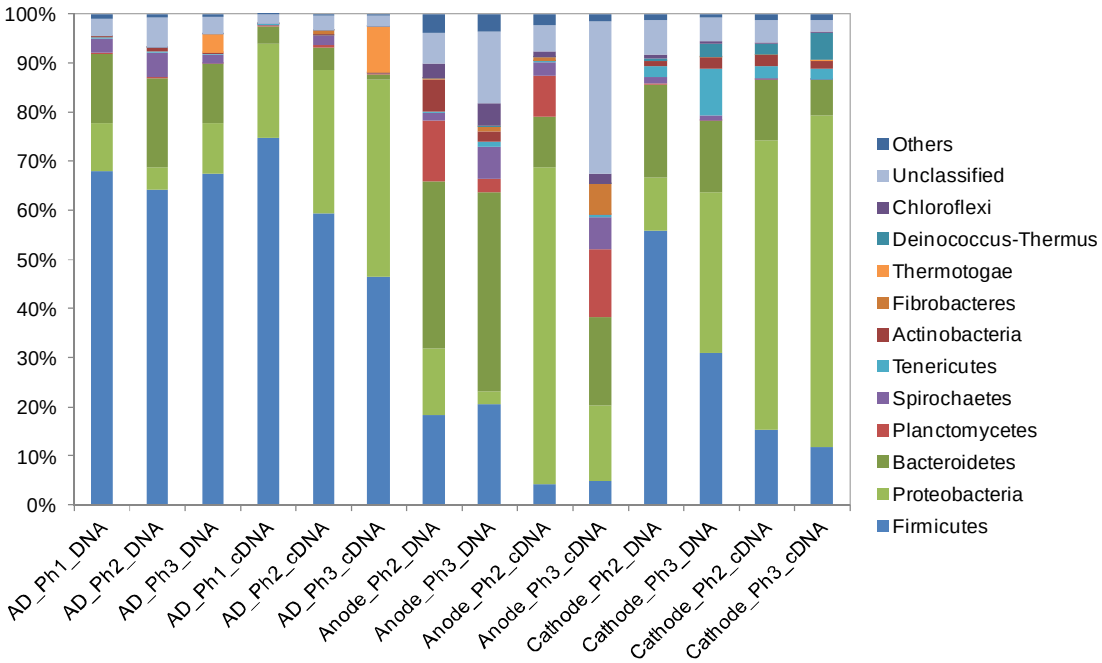

b)

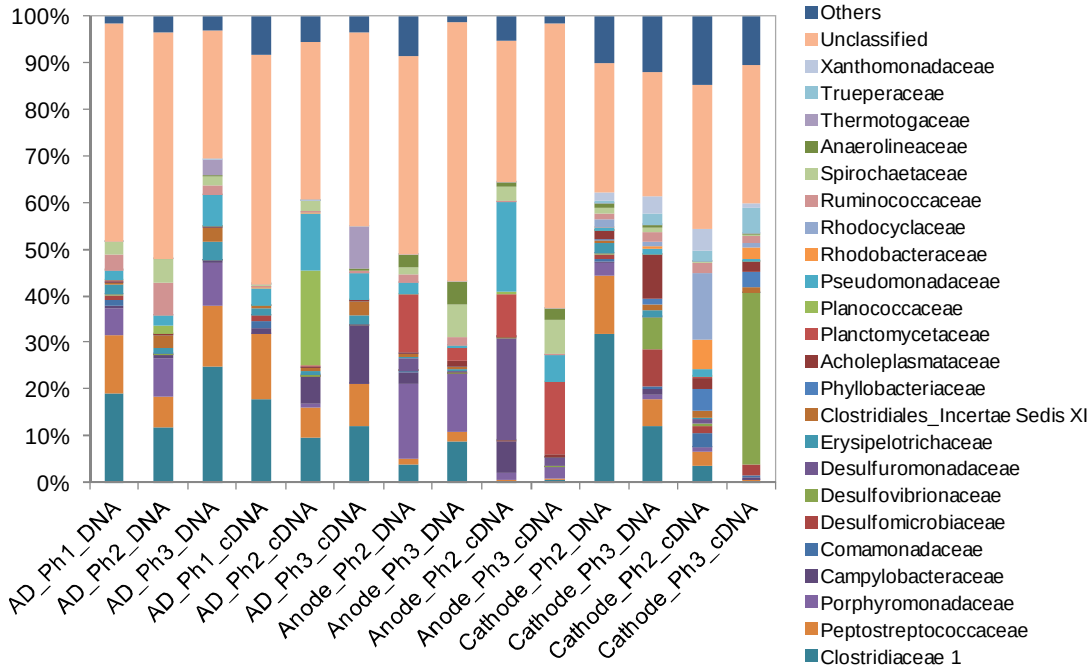

c)

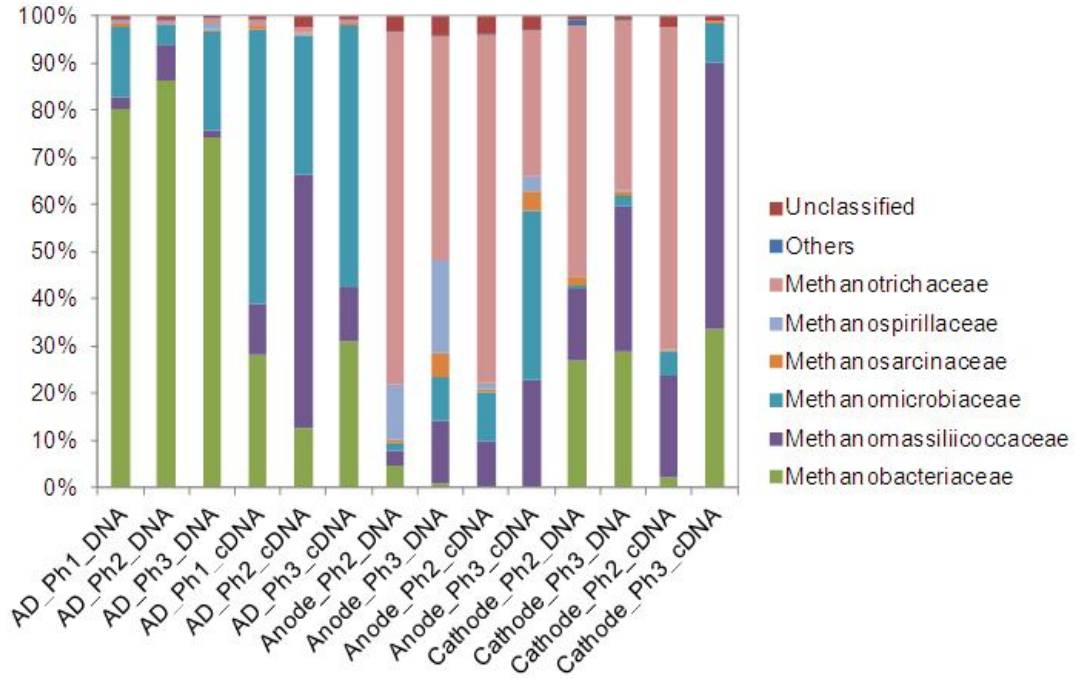

Figure 5 Taxonomic assignment of sequencing reads from Eubacterial community of the AD effluent at the end of Phases 1, 2 and 3, and the biofilm harboured on the anode and cathode of the MEC at the end of Phase 2 and 3 for DNA and cDNA, at a) phylum b) family levels; and c) for Archaeal community at family level. Relative abundance was defined as the number of reads (sequences) affiliated with any given taxon divided by the total number of reads per sample. Phylogenetic groups with relative abundance lower than 1% were categorized as "others".

3.6.3. Biodiversity analysis

Table 4 shows the results for the biodiversity analysis performed on the AD samples and the anode and cathode biofilms of the MEC samples. The Inverted Simpson and Shannon indexes of the AD samples for eubacteria at DNA level decreased during Phase 2 and recovered in Phase 3, showing the opposite behaviour for archaea. The biodiversity of the bioanode and the biocathode increased regarding archaeal population, either in total (DNA) or in metabolically active (cDNA). On the contrary, eubacteria decreased its biodiversity, result that agrees with the trend observed in other studies [77].

Table 4. Diversity indexes for Eubacteria and Archaea community of the AD effluent at the end of Phases 1, 2 and 3, and the biofilm harboured on the anode and cathode of the MEC at the end of Phase 2 and 3 for DNA and cDNA samples (mean±standard deviation). Normalised to the lowest number of reads (56424 and 59671 for eubacteria and archaea, respectively).

	Reads	Inverted Simpson	Shannon
Eubacteria			
ADPh1-DNA	116316	14.67±0.07	3.94±0.01
ADPh2-DNA	142940	13.00±0.07	3.85±0.01
ADPh3-DNA	117089	13.61±0.08	4.02±0.01
Anodei-DNA	95391	38.16±0.22	4.90±0.01
Anodef-DNA	96879	34.12±0.20	4.87±0.01
Cathodei-DNA	65906	16.12±0.06	4.29±0.00
Cathodef-DNA	61741	35.48±0.09	4.57±0.00
ADPh1-cDNA	163191	7.55±0.03	3.07±0.01
ADPh2-cDNA	152610	7.26±0.04	3.39±0.01
ADPh3-cDNA	214052	6.54±0.03	2.78±0.01
Anodei-cDNA	147740	8.58±0.05	3.71±0.01
Anodef-cDNA	171251	9.24±0.05	3.54±0.01
Cathodei-cDNA	56424	3.65±0.00	4.53±0.00
Cathodef-cDNA	93469	5.22±0.02	3.01±0.01
Archaea			
ADPh1-DNA	97511	2.87±0.01	1.67±0.01
ADPh2-DNA	59777	3.41±0.00	2.10±0.00
ADPh3-DNA	71736	3.33±0.01	1.84±0.00
Anodei-DNA	183422	1.58±0.00	1.18±0.01
Anodef-DNA	140800	2.83±0.01	1.90±0.01
Cathodei-DNA	220361	1.77±0.01	1.44±0.01
Cathodef-DNA	92290	4.92±0.02	2.40±0.01
ADPh1-cDNA	59671	3.95±0.00	2.26±0.00
ADPh2-cDNA	82628	5.97±0.02	2.61±0.00
ADPh3-cDNA	91203	6.75±0.02	2.54±0.00
Anodei-cDNA	125143	2.02±0.01	1.60±0.01
Anodef-cDNA	99696	6.35±0.02	2.55±0.01
Cathodei-cDNA	99324	2.37±0.01	1.76±0.01
Cathodef-cDNA	64740	4.61±0.01	2.23±0.00

3.6.4 Correspondence analysis

Correspondence analysis results for eubacteria and archaea community are shown in Figure 6a and 6b, respectively. Regarding eubacteria, AD samples were clustered together, especially in the case of DNA, while for cDNA form the samples were more disperse and detached from the first ones. This cluster included the Phase 2 DNA sample of the cathode biofilm, which separated lately at the end of the assay. When looking at the Phase 2 cathode sample for active microorganisms (cDNA), it was nearer to the anode samples, although the Phase 3 sample differentiated completely from all the samples analysed. Finally, the anode samples clustered clearly in two groups, one for DNA and a second one for cDNA, showing that the metabolically active population (cDNA sequencing) was different from total population (DNA sequencing).

Archaeal results for the AD biomass showed that the three DNA samples were prochain, so little differences in composition were detected between inhibited and stable states. On the contrary, cDNA samples, related to the active microorganisms, were distant from DNA samples and Phase 1 and 3 samples were clustered together while Phase 2 sample moved away from them. This means that active microorganisms in the initial sample shifted to a different active community during Phase 2 due to the inhibition and, once recovered with the recirculation loop, went back to the previous composition. Regarding the anode and cathode communities, Phase 2 DNA and cDNA samples resembled and an evolution was observed for the Phase 3 samples, moving away from the initial composition, especially for cDNA. Interestingly, the biocathode cDNA Phase 3 sample approached to the cDNA AD sample of Phase 2, suggesting that the active population of the cathode resembled the AD population under inhibition.

a)

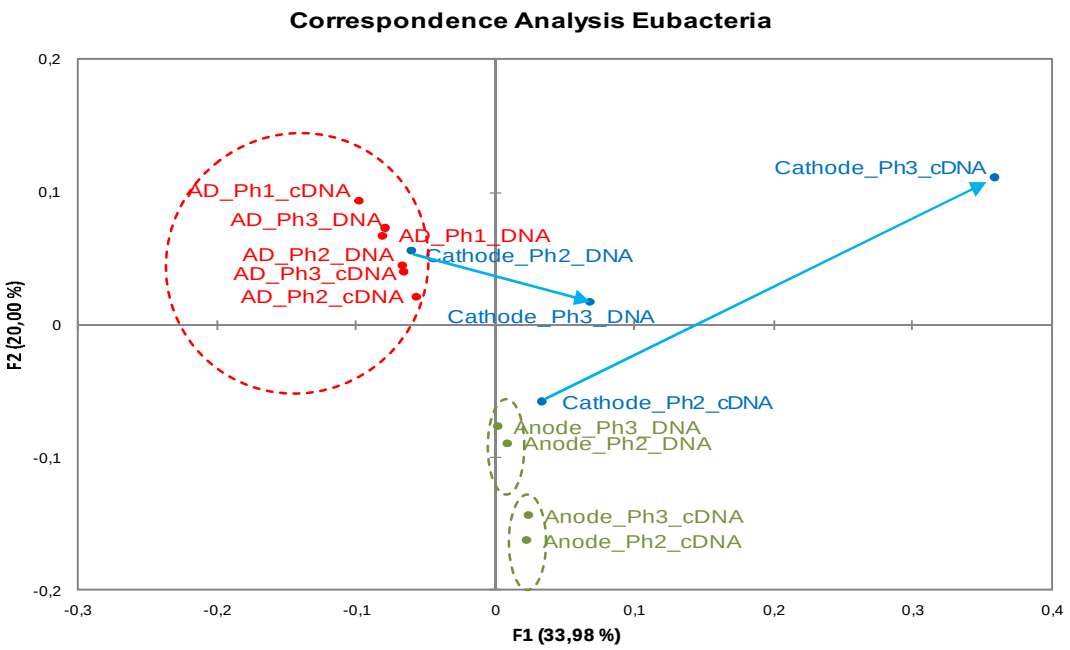

b)

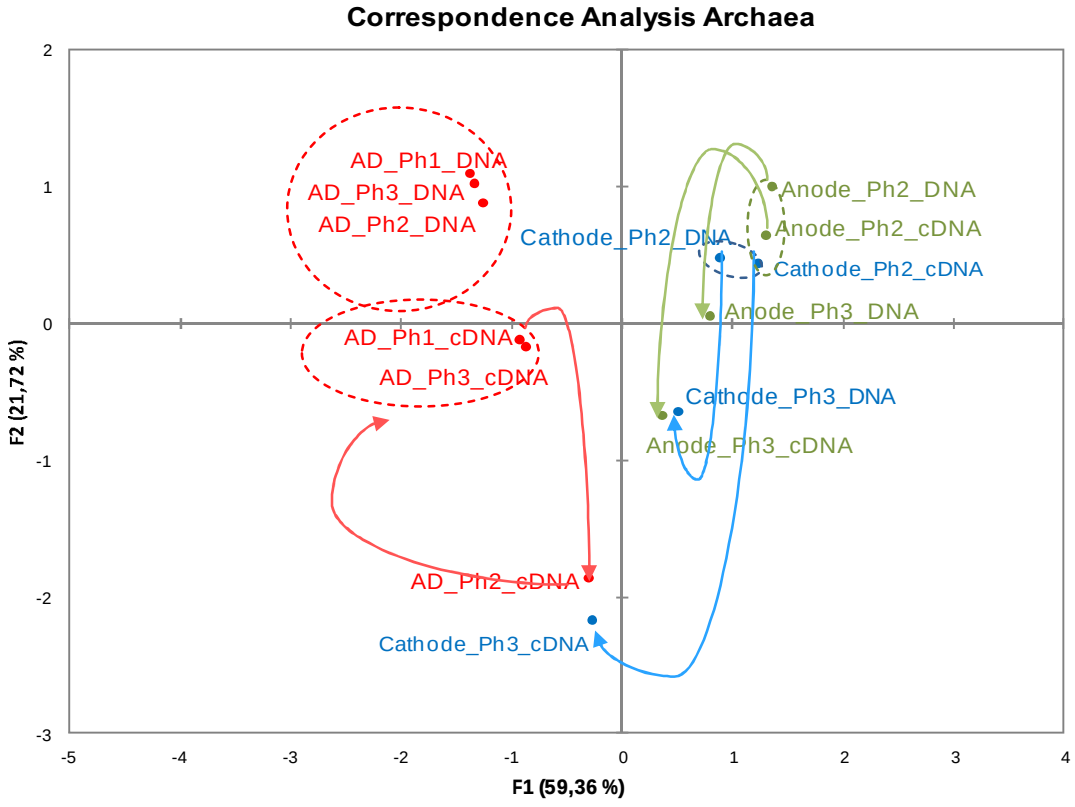

Figure 6 Correspondence Analysis of the AD effluent at the end of Phases 1, 2 and 3, and the biofilm harboured on the anode and cathode of the MEC at the end of Phase 2 and 3 for DNA and cDNA samples regarding (a) Eubacteria and (b) Archaea community.

4. Conclusions

The integration of anaerobic digestion (AD) and a microbial electrolysis cell (MEC) with a methanogenic biocathode has proven to be a promising strategy to treat high strength wastewaters with a multiple purpose. The methane production of the AD could be recovered after the inhibition of the reactor due to the doubling of the organic and nitrogen loading rate thanks to the connexion of a recirculation loop with the MEC. Ammonium removal in the anode compartment of the MEC achieved 14.46 g $N\text{-}NH_4^+$ m^{-2} d^{-1}, while obtaining on average 79 L CH_4 m^{-3} d^{-1} through the conversion of CO_2 in the cathode compartment. The microbial analysis showed that methylotrophic *Methanossiliicoccaceae* family (*Methanomassiliicoccus* genus) was the most abundant among active archaea in the AD during the inhibited state. On the other hand, in the cathode *Methanobacteriaceae* family (*Methanobrevibacter* and *Methanobacterium* genera), usually found to be the most abundant in methanogenic biocathodes, shared dominance with *Methanomassiliicoccaceae* (*Methanomassiliicoccus* genus) and *Methanotrichaceae* (*Methanothrix* genus) families.

Acknowledgements

The authors would like to acknowledge the valuable contribution to this work of Miriam Guivernau (GIRO Joint Research Unit IRTA-UPC), for the implementation of the protocols of RT-qPCR and simultaneous DNA and RNA extraction with cDNA synthesis. This research was funded by the Spanish Ministry of Economy and Competitiveness (INIA projects RTA2012-00096-00-00 and RTA2015-00079-C02-01) and the CERCA Programme (Generalitat de Catalunya). The first author was supported by a PhD grant from the Secretariat for Universities and Research of the Ministry of Economy and Knowledge of the Catalan Government (pre-doctoral grant 2013FI_B 00014).

606 **References**

607 [1] Schiermeier Q, Tollefson J, Scully T, Witze A, Morton O. Electricity without carbon. Nature.
608 2008;454:816-23.

609 [2] Forster-Carneiro T, Berni MD, Dorileo IL, Rostagno MA. Biorefinery study of availability of
610 agriculture residues and wastes for integrated biorefineries in Brazil. Resources, Conservation and
611 Recycling. 2013;77:78-88.

612 [3] Pan S-Y, Du MA, Huang IT, Liu IH, Chang EE, Chiang P-C. Strategies on implementation of
613 waste-to-energy (WTE) supply chain for circular economy system: a review. Journal of Cleaner
614 Production. 2015;108, Part A:409-21.

615 [4] Rózsenberszki T, Koók L, Bakonyi P, Nemestóthy N, Logroño W, Pérez M, Urquizo G, Recalde
616 C, Kurdi R, Sarkady A. Municipal waste liquor treatment via bioelectrochemical and fermentation
617 (H_2 + CH_4) processes: Assessment of various technological sequences. Chemosphere.
618 2017;171:692-701.

619 [5] Premier GC, Kim JR, Massanet-Nicolau J, Kyazze G, Esteves SRR, Penumathsa BKV,
620 Rodríguez J, Maddy J, Dinsdale RM, Guwy AJ. Integration of biohydrogen, biomethane and
621 bioelectrochemical systems. Renewable Energy. 2013;49:188-92.

622 [6] Sadhukhan J, Lloyd JR, Scott K, Premier GC, Yu EH, Curtis T, Head IM. A critical review of
623 integration analysis of microbial electrosynthesis (MES) systems with waste biorefineries for the
624 production of biofuel and chemical from reuse of CO_2. Renewable and Sustainable Energy
625 Reviews. 2016;56:116-32.

626 [7] Lu L, Ren ZJ. Microbial electrolysis cells for waste biorefinery: A state of the art review.
627 Bioresour Technol. 2016;215:254-64.

628 [8] Oliot M, Galier S, Roux de Balmann H, Bergel A. Ion transport in microbial fuel cells: Key roles,
629 theory and critical review. Applied Energy. 2016;183:1682-704.

630 [9] Rodríguez Arredondo M, Kuntke P, ter Heijne A, Hamelers HVM, Buisman CJN. Load ratio
631 determines the ammonia recovery and energy input of an electrochemical system. Water Res.
632 2017;111:330-7.

633 [10] Zhang X, Zhu F, Chen L, Zhao Q, Tao G. Removal of ammonia nitrogen from wastewater
634 using an aerobic cathode microbial fuel cell. Bioresour Technol. 2013;146:161-8.
635 [11] Kuntke P, Smiech KM, Bruning H, Zeeman G, Saakes M, Sleutels THJA, Hamelers HVM,
636 Buisman CJN. Ammonium recovery and energy production from urine by a microbial fuel cell.
637 Water Res. 2012;46:2627-36.
638 [12] Sotres A, Cerrillo M, Viñas M, Bonmatí A. Nitrogen recovery from pig slurry in a two-
639 chambered bioelectrochemical system. Bioresour Technol. 2015;194:373-82.
640 [13] Cerrillo M, Oliveras J, Viñas M, Bonmatí A. Comparative assessment of raw and digested pig
641 slurry treatment in bioelectrochemical systems. Bioelectrochemistry. 2016;110:69-78.
642 [14] Kuntke P, Sleutels THJA, Saakes M, Buisman CJN. Hydrogen production and ammonium
643 recovery from urine by a Microbial Electrolysis Cell. Int J Hydrogen Energy. 2014;39:4771-8.
644 [15] Liu Y, Qin M, Luo S, He Z, Qiao R. Understanding ammonium transport in bioelectrochemical
645 systems towards its recovery. Scientific Reports. 2016;6:22547.
646 [16] Ge Z, Zhang F, Grimaud J, Hurst J, He Z. Long-term investigation of microbial fuel cells
647 treating primary sludge or digested sludge. Bioresour Technol. 2013;136:509-14.
648 [17] Durruty I, Bonanni PS, González JF, Busalmen JP. Evaluation of potato-processing
649 wastewater treatment in a microbial fuel cell. Bioresour Technol. 2012;105:81-7.
650 [18] Cerrillo M, Viñas M, Bonmatí A. Microbial fuel cells for polishing effluents of anaerobic
651 digesters under inhibition, due to organic and nitrogen overloads. J Chem Technol Biotechnol.
652 2017.
653 [19] Cerrillo M, Viñas M, Bonmatí A. Removal of volatile fatty acids and ammonia recovery from
654 unstable anaerobic digesters with a microbial electrolysis cell. Bioresour Technol. 2016;219:348-
655 56.
656 [20] Fradler KR, Kim JR, Shipley G, Massanet-Nicolau J, Dinsdale RM, Guwy AJ, Premier GC.
657 Operation of a bioelectrochemical system as a polishing stage for the effluent from a two-stage
658 biohydrogen and biomethane production process. Biochemical Engineering Journal. 2014;85:125-
659 31.

660 [21] Tugtas AE, Cavdar P, Calli B. Bio-electrochemical post-treatment of anaerobically treated
661 landfill leachate. Bioresour Technol. 2013;128:266-72.
662 [22] Kim T, An J, Jang JK, Chang IS. Coupling of anaerobic digester and microbial fuel cell for
663 COD removal and ammonia recovery. Bioresour Technol. 2015;195:217-22.
664 [23] Schievano A, Sciarria TP, Gao YC, Scaglia B, Salati S, Zanardo M, Quiao W, Dong R, Adani
665 F. Dark fermentation, anaerobic digestion and microbial fuel cells: An integrated system to valorize
666 swine manure and rice bran. Waste Management. 2016;56:519-29.
667 [24] Zhang Y, Angelidaki I. Counteracting ammonia inhibition during anaerobic digestion by
668 recovery using submersible microbial desalination cell. Biotechnol Bioeng. 2015;112:1478-82.
669 [25] Cerrillo M, Viñas M, Bonmatí A. Overcoming organic and nitrogen overload in thermophilic
670 anaerobic digestion of pig slurry by coupling a microbial electrolysis cell. Bioresour Technol.
671 2016;216:362-72.
672 [26] Song Y-C, Feng Q, Ahn Y. Performance of the bio-electrochemical anaerobic digestion of
673 sewage sludge at different hydraulic retention times. Energy Fuels. 2016;30:352-9.
674 [27] Ran Z, Gefu Z, Kumar JA, Chaoxiang L, Xu H, Lin L. Hydrogen and methane production in a
675 bio-electrochemical system assisted anaerobic baffled reactor. Int J Hydrogen Energy.
676 2014;39:13498-504.
677 [28] Zhen G, Kobayashi T, Lu X, Kumar G, Xu K. Biomethane recovery from *Egeria densa* in a
678 microbial electrolysis cell-assisted anaerobic system: Performance and stability assessment.
679 Chemosphere. 2016;149:121-9.
680 [29] Xu H, Wang K, Holmes DE. Bioelectrochemical removal of carbon dioxide (CO_2): An
681 innovative method for biogas upgrading. Bioresour Technol. 2014;173:392-8.
682 [30] Batlle-Vilanova P, Puig S, Gonzalez-Olmos R, Vilajeliu-Pons A, Balaguer MD, Colprim J.
683 Deciphering the electron transfer mechanisms for biogas upgrading to biomethane within a mixed
684 culture biocathode. RSC Advances. 2015;5:52243-51.
685 [31] Ryckebosch E, Drouillon M, Vervaeren H. Techniques for transformation of biogas to
686 biomethane. Biomass and Bioenergy. 2011;35:1633-45.

687 [32] Cheng S, Xing D, Call DF, Logan BE. Direct biological conversion of electrical current into
688 methane by electromethanogenesis. Environmental Science & Technology. 2009;43:3953-8.
689 [33] Villano M, Monaco G, Aulenta F, Majone M. Electrochemically assisted methane production in
690 a biofilm reactor. J Power Sources. 2011;196:9467-72.
691 [34] Van Eerten-Jansen MCAA, Veldhoen AB, Plugge CM, Stams AJM, Buisman CJN, Ter Heijne
692 A. Microbial community analysis of a methane-producing biocathode in a bioelectrochemical
693 system. Archaea. 2013;2013:12.
694 [35] Bo T, Zhu X, Zhang L, Tao Y, He X, Li D, Yan Z. A new upgraded biogas production process:
695 Coupling microbial electrolysis cell and anaerobic digestion in single-chamber, barrel-shape
696 stainless steel reactor. Electrochemistry Communications. 2014;45:67-70.
697 [36] Gajaraj S, Huang Y, Zheng P, Hu Z. Methane production improvement and associated
698 methanogenic assemblages in bioelectrochemically assisted anaerobic digestion. Biochemical
699 Engineering Journal. 2017;117, Part B:105-12.
700 [37] Liu W, Cai W, Guo Z, Wang L, Yang C, Varrone C, Wang A. Microbial electrolysis contribution
701 to anaerobic digestion of waste activated sludge, leading to accelerated methane production.
702 Renewable Energy. 2016;91:334-9.
703 [38] Yin Q, Zhu X, Zhan G, Bo T, Yang Y, Tao Y, He X, Li D, Yan Z. Enhanced methane production
704 in an anaerobic digestion and microbial electrolysis cell coupled system with co-cultivation of
705 Geobacter and Methanosarcina. Journal of Environmental Sciences. 2016;42:210-4.
706 [39] Hou Y, Zhang R, Luo H, Liu G, Kim Y, Yu S, Zeng J. Microbial electrolysis cell with spiral
707 wound electrode for wastewater treatment and methane production. Process Biochemistry.
708 2015;50:1103-9.
709 [40] Zeppilli M, Villano M, Aulenta F, Lampis S, Vallini G, Majone M. Effect of the anode feeding
710 composition on the performance of a continuous-flow methane-producing microbial electrolysis
711 cell. Environmental Science and Pollution Research. 2015;22:7349-60.
712 [41] Marshall CW, Ross DE, Fichot EB, Norman RS, May HD. Electrosynthesis of commodity
713 chemicals by an autotrophic microbial community. Appl Environ Microbiol. 2012;78:8412-20.

714 [42] Zhen G, Kobayashi T, Lu X, Xu K. Understanding methane bioelectrosynthesis from carbon
715 dioxide in a two-chamber microbial electrolysis cells (MECs) containing a carbon biocathode.
716 Bioresour Technol. 2015;186:141-8.
717 [43] Sotres A, Cerrillo M, Viñas M, Bonmatí A. Nitrogen removal in a two-chambered MFC:
718 establishment of a nitrifying-denitrifying microbial community on an intermittent aerated cathode.
719 Chemical Engineering Journal. 2016;284:905-16.
720 [44] Cerrillo M, Morey L, Viñas M, Bonmatí A. Assessment of active methanogenic archaea in a
721 methanol-fed upflow anaerobic sludge blanket reactor. Appl Microbiol Biotechnol. 2016;100:10137-
722 46.
723 [45] Lu H, Oehmen A, Virdis B, Keller J, Yuan Z. Obtaining highly enriched cultures of *Candidatus*
724 *Accumulibacter* phosphates through alternating carbon sources. Water Res. 2006;40:3838-48.
725 [46] APHA. Standard methods for the examination of water and wastewater. 20th ed. Washington,
726 D.C.: American Public Health Association, American Water Works Association, and Water
727 Pollution Control Federation; 1999.
728 [47] Alberto MCR, Arah JRM, Neue HU, Wassmann R, Lantin RS, Aduna JB, Bronson KF. A
729 sampling technique for the determination of dissolved methane in soil solution. Chemosphere -
730 Global Change Science. 2000;2:57-63.
731 [48] Ripley LE, Boyle WC, Converse JC. Improved alkalimetric monitoring for anaerobic digestion
732 of high-strength wastes. Journal (Water Pollution Control Federation). 1986;58:406-11.
733 [49] Bernard O, Polit M, Hadj-Sadok Z, Pengov M, Dochain D, Estaben M, Labat P. Advanced
734 monitoring and control of anaerobic wastewater treatment plants: software sensors and controllers
735 for an anaerobic digester. Water Science Technology. 2001;43:175-82.
736 [50] Cerrillo M, Viñas M, Bonmatí A. Unravelling the active microbial community in a thermophilic
737 anaerobic digester-microbial electrolysis cell coupled system under different conditions. Water
738 Res. 2016;110:192-201.
739 [51] Wang Q, Garrity GM, Tiedje JM, Cole JR. Naïve bayesian classifier for rapid assignment of
740 rRNA sequences into the new bacterial taxonomy. Appl Environ Microbiol. 2007;73:5261-7.

741 [52] Schloss PD, Westcott SL, Ryabin T, Hall JR, Hartmann M, Hollister EB, Lesniewski RA,
742 Oakley BB, Parks DH, Robinson CJ, Sahl JW, Stres B, Thallinger GG, Van Horn DJ, Weber CF.
743 Introducing mothur: open-source, platform-independent, community-supported software for
744 describing and comparing microbial communities. Appl Environ Microbiol. 2009;75:7537-41.
745 [53] Zhang X, He W, Ren L, Stager J, Evans PJ, Logan BE. COD removal characteristics in air-
746 cathode microbial fuel cells. Bioresour Technol. 2015;176:23-31.
747 [54] Catal T, Cysneiros D, O'Flaherty V, Leech D. Electricity generation in single-chamber
748 microbial fuel cells using a carbon source sampled from anaerobic reactors utilizing grass silage.
749 Bioresour Technol. 2011;102:404-10.
750 [55] Min B, Kim J, Oh S, Regan JM, Logan BE. Electricity generation from swine wastewater using
751 microbial fuel cells. Water Res. 2005;39:4961-8.
752 [56] Liu H, Ramnarayanan R, Logan BE. Production of electricity during wastewater treatment
753 using a single chamber microbial fuel cell. Environmental Science & Technology. 2004;38:2281-5.
754 [57] Villano M, Scardala S, Aulenta F, Majone M. Carbon and nitrogen removal and enhanced
755 methane production in a microbial electrolysis cell. Bioresour Technol. 2013;130:366-71.
756 [58] Geppert F, Liu D, van Eerten-Jansen M, Weidner E, Buisman C, ter Heijne A.
757 Bioelectrochemical power-to-gas: State of the art and future perspectives. Trends in
758 Biotechnology. 2016;34:879-94.
759 [59] Van Eerten-Jansen MCAA, Heijne AT, Buisman CJN, Hamelers HVM. Microbial electrolysis
760 cells for production of methane from CO2: long-term performance and perspectives. International
761 Journal of Energy Research. 2012;36:809-19.
762 [60] Blasco-Gómez R, Batlle-Vilanova P, Villano M, Balaguer M, Colprim J, Puig S. On the edge of
763 research and technological application: a critical review of electromethanogenesis. International
764 Journal of Molecular Sciences. 2017;18:874.
765 [61] Petersson A, Wellinger A. Biogas upgrading technologies – developments and innovations.
766 IEA Bioenergy; 2009.
767 [62] Maurer M, Schwegler P, Larsen TA. Nutrients in urine: energetic aspects of removal and
768 recovery. Water Sci Technol. 2003;48:37-46.

769 [63] Zhang C, Yuan Q, Lu Y. Inhibitory effects of ammonia on methanogen *mcrA* transcripts in
770 anaerobic digester sludge. FEMS Microbiology Ecology. 2014;87:368-77.
771 [64] Angelidaki I, Ahring BK. Thermophilic anaerobic digestion of livestock waste: the effect of
772 ammonia. Appl Microbiol Biotechnol. 1993;38:560-4.
773 [65] Hansen KH, Angelidaki I, Ahring BK. Anaerobic digestion of swine manure: inhibition by
774 ammonia. Water Res. 1998;32:5-12.
775 [66] Tuan NN, Chang YC, Yu CP, Huang SL. Multiple approaches to characterize the microbial
776 community in a thermophilic anaerobic digester running on swine manure: a case study.
777 Microbiological Research. 2014;169:717-24.
778 [67] Bonmatí A, Sotres A, Mu Y, Rozendal RA, Rabaey K. Oxalate degradation in a
779 bioelectrochemical system: Reactor performance and microbial community characterization.
780 Bioresour Technol. 2013;143:147-53.
781 [68] Sotres A, Díaz-Marcos J, Guivernau M, Illa J, Magrí A, Prenafeta-Boldú FX, Bonmatí A, Viñas
782 M. Microbial community dynamics in two-chambered microbial fuel cells: effect of different ion
783 exchange membranes. Journal of Chemical Technology & Biotechnology. 2015;90:1497-506.
784 [69] Dridi B, Fardeau M-L, Ollivier B, Raoult D, Drancourt M. *Methanomassiliicoccus luminyensis*
785 gen. nov., sp. nov., a methanogenic archaeon isolated from human faeces. International Journal of
786 Systematic and Evolutionary Microbiology. 2012;62:1902-7.
787 [70] Borrel G, O'Toole PW, Harris HMB, Peyret P, Brugère J-F, Gribaldo S. Phylogenomic data
788 support a seventh order of methylotrophic methanogens and provide insights into the evolution of
789 methanogenesis. Genome Biology and Evolution. 2013;5:1769-80.
790 [71] Moestedt J, Müller B, Westerholm M, Schnürer A. Ammonia threshold for inhibition of
791 anaerobic digestion of thin stillage and the importance of organic loading rate. Microbial
792 Biotechnology. 2016;9:180-94.
793 [72] Hori T, Haruta S, Sasaki D, Hanajima D, Ueno Y, Ogata A, Ishii M, Igarashi Y. Reorganization
794 of the bacterial and archaeal populations associated with organic loading conditions in a
795 thermophilic anaerobic digester. Journal of Bioscience and Bioengineering. 2015;119:337-44.

796 [73] Cai W, Liu W, Yang C, Wang L, Liang B, Thangavel S, Guo Z, Wang A. Biocathodic
797 methanogenic community in an integrated anaerobic digestion and microbial electrolysis system
798 for enhancement of methane production from waste sludge. ACS Sustainable Chemistry &
799 Engineering. 2016;4:4913-21.
800 [74] Rotaru A-E, Shrestha PM, Liu F, Shrestha M, Shrestha D, Embree M, Zengler K, Wardman C,
801 Nevin KP, Lovley DR. A new model for electron flow during anaerobic digestion: direct interspecies
802 electron transfer to *Methanosaeta* for the reduction of carbon dioxide to methane. Energy &
803 Environmental Science. 2014;7:408-15.
804 [75] Taher E, Chandran K. High-rate, high-yield production of methanol by ammonia-oxidizing
805 bacteria. Environmental Science & Technology. 2013;47:3167-73.
806 [76] Ge X, Yang L, Sheets JP, Yu Z, Li Y. Biological conversion of methane to liquid fuels: Status
807 and opportunities. Biotechnology Advances. 2014;32:1460-75.
808 [77] Siegert M, Yates MD, Spormann AM, Logan BE. *Methanobacterium* dominates biocathodic
809 archaeal communities in methanogenic microbial electrolysis cells. ACS Sustainable Chemistry &
810 Engineering. 2015;3:1668-76.
811
812